Quantitative Analysis of Myocardial Structure in Insulin-Dependent Diabetes Mellitus: Effects of Immediate and Delayed Insulin Replacement (43710)

ED W. THOMPSON[1]
Department of Biology, Winona State University, Winona, Minnesota 55987–5838

Abstract. **The effects of severe, chronic diabetes mellitus and of immediate or delayed insulin replacement on the different components of the myocardium and cardiocytes were quantified and correlated. A significant decrease in cardiocyte cross-sectional area occurred during the first 12 weeks of diabetes and then stabilized. This was accompanied by decreases in the relative volume densities (RVDs) of myofibrils and mitochondria, resulting in absolute loss of more than 40% of each of these cellular components after 26 weeks of diabetes. Interstitial and perivascular deposition of extracellular matrix produced a tripling of its RVD in the myocardium over 26 weeks of diabetes at the expense of both cardiocytes and capillaries. Capillary density and diameter also exhibited progressive decreases of more than 20% over 26 weeks of diabetes. Insulin treatment which maintained euglycemia and restored normal growth prevented this structural pathology when begun three days after induction of diabetes. When delayed for 12 weeks, insulin reversed the changes in cardiocyte and capillary RVD, and in capillary diameter within 6 weeks, ultrastructural changes within 12 weeks, and cardiocyte cross-sectional area after 26 weeks. However, even after 26 weeks of treatment, the extracellular matrix remained more than twice that observed in nondiabetic animals, with a consequent decrease in the number of capillaries per unit volume of tissue. This study demonstrates that diabetes produces a progressive, marked disorganization of the myocardium which can be prevented, but only selectively reversed, by insulin treatment. These structural changes are relevant to the functional changes which occur in diabetic cardiomyopathy.** [P.S.E.B.M. 1994, Vol 205]

Heart disease remains one of the most serious sequelae of diabetes mellitus, even with good control of blood glucose levels. Although this was initially attributed almost entirely to accelerated coronary atherosclerosis, it soon became well recognized from epidemiologic (1), clinical (2, 3), biopsy (5, 6), and postmortem (2, 7) evidence that a diabetic cardiomyopathy independent of vascular disease also plays a major role. Contractile dysfunction can often be detected in diabetic patients before the symptoms of heart disease present clinically (3, 6), but, in other instances, may not become evident except under conditions of increased stress (4, 8, 9). Cardiac contractile abnormalities in diabetic animal models parallel those observed in the human population (10, 11).

A major component of this diabetic cardiomyopathy involves abnormalities in myocardial composition and structure which arise from the altered biochemical milieu and subsequently underlie many of the contractile and hemodynamic dysfunctions which lead to pump failure. Progressive accumulations of collagen and glycoproteins in the myocardial extracellular matrix are consistent findings in both diabetic patients (2, 7) and experimentally diabetic animals (12, 13), and are related to the decreased compliance of this tissue (2, 14). Ultrastructural examinations have revealed marked abnormalities of the cardiomyocytes in severely diabetic animals (15–17), but mildly diabetic an-

[1] To whom requests for reprints should be addressed at Department of Biology, Winona State University, P.O. Box 5838, Winona, MN 55987–5838.

Received July 19, 1993. [P.S.E.B.M. 1994, Vol 205]
Accepted December 8, 1993.

0037-9727/94/2054–0294$10.50/0

imals typically show little or no ultrastructural damage (18, 19). Thickening or reduplication of capillary basement membranes in the diabetic myocardium have been frequently (5, 6, 13), although not always (17), observed.

It is not clear, however, how quickly and to what extent the various components of the tissue or cardiocytes are affected, nor is it clear what effect intervention with insulin might have on this disorder. We demonstrated (13, 19) in the rat myocardium that structural changes at both the light and electron microscopic levels occur in a focal pattern, with both the size and number of affected areas increasing with the duration of diabetes. After six months, more than half of the tissue showed altered morphology. We also noted that insulin treatment begun after twelve weeks of diabetes, when many changes were already present, could significantly but not completely reverse them.

In the present study, I have extended these observations by using stereology and quantitative morphometry to define the pattern of changes in the diabetic myocardium and to compare the effects of early and late insulin replacement.

Materials and Methods

Experimental Animals. Diabetes was induced in young male Sprague-Dawley rats by intravenous injection of 55 mg/kg alloxan monohydrate (Sigma, St. Louis, MO). Control rats received equivalent doses of sterile saline. Plasma glucose concentrations were measured three days later and biweekly thereafter. All animals were weighed weekly and urine concentrations of glucose, ketones, and protein were estimated by dipstick (Boehringer Mannheim, Indianapolis, IN). Each animal was assigned to an experimental group at the time of injection to eliminate selection bias due to spontaneous mortality.

Only rats with plasma glucose values above 300 mg/dl (17 m*M*) and gaining little or no weight were considered seriously insulin deficient (13, 19, 20) and included in this study. Marked glucosuria and ketonuria were also characteristic of the diabetes. These criteria effectively limited the study to the more severe end of the spectrum of diabetes, minimizing variations due to differences in severity of the disease which we have shown to be significant factors in the development of myocardial sequelae (19). Previous experience (13, 19–21) has demonstrated that more than two-thirds of the animals injected with alloxan will meet these criteria yet survive for the intervals in this study.

Insulin treatment followed two protocols when used. In the first, to determine if it could prevent the degenerative myocardial changes of diabetes, treatment began three days after injection of alloxan (Insulin Treatment–Prevention; ITP). In the second, treatment of diabetic animals was delayed for 12 weeks to determine if insulin replacement could reverse changes which had already occurred (Insulin Treatment–Reversal; ITR). Under either protocol, treatment consisted of a mixture of two units each of regular and NPH insulins (Eli Lilly Co., Indianapolis, IN) injected subcutaneously every 12 hr in a rotating pattern of six sites on the back and abdomen (13, 21). Age-matched control (diabetic) rats received equal volumes of saline. Successful insulin treatment was indicated by blood glucose levels between 70 and 140 mg/dl (3.9–7.8 m*M*) and resumption of normal weight gain. In a pilot experiment to verify that this treatment protocol maintained euglycemia throughout the day (Fig. 1), we measured blood glucose and urine glucose and ketones over a 24-hr period in groups of age-matched, untreated and insulin-treated diabetic rats ($n = 4$ per group).

Throughout the study, all animals were housed individually within an AAALAC-accredited facility and had free access to food and water. Strong efforts were taken to minimize or eliminate any unnecessary discomfort of the experimental animals. Any diabetic rat which stopped eating or drinking, became lethargic, showed a sudden or significant weight loss, or developed renal failure was immediately euthanized with carbon dioxide. All sacrifice for collection of tissue was carried out under full pentobarbital anesthesia as described below.

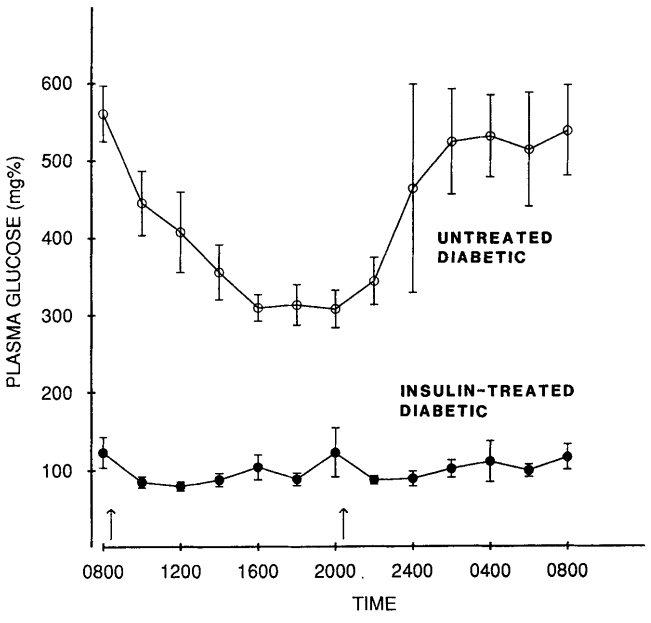

Figure 1. Plasma glucose levels measured every 2 hr in age-matched untreated (○—○) and insulin-treated (●—●) diabetic rats confirm that insulin treatment maintained consistent euglycemia in contrast to the markedly elevated and fluctuating values in diabetes. Each group consisted of four rats, and all values are expressed as $\bar{x} \pm$ SD. Arrows indicate times of semi-daily insulin injections.

Sacrifice and Tissue Preparation. After intervals of six, 12, or 26 weeks of diabetes, or after the same periods of insulin treatment following either of the protocols noted above, each control or experimental animal was fully anesthetized by intraperitoneal injection of sodium pentobarbital, 65 mg/kg. The heart was rapidly excised, rinsed three times in ice-cold saline, and mounted on the tip of a retrograde aortic perfusion apparatus. The coronary vasculature was flushed of blood and the heart arrested in diastole by brief perfusion with 25 m*M* potassium phosphate buffer, pH 7.35, containing 90 m*M* NaCl, 25 m*M* KCl, and saturated with oxygen by constant bubbling. The heart was then perfused for 10 min with 2% glutaraldehyde and 2% paraformaldehyde in 0.1 *M* sodium cacodylate buffer, pH 7.35, containing 50 m*M* KCl and 5 m*M* $CaCl_2$, also saturated with oxygen. Perfusion was gravity driven at a pressure of 120 mm Hg and in all cases began within 60 sec of thoracotomy.

The atria and valves of each heart were trimmed away and discarded, and the right ventricular free wall was separated from the septum and left ventricular wall. Both were weighed and returned to fresh fixative for an additional 8–24 hr. The midregion of the left ventricular anterior papillary muscle was further divided, postfixed in osmium, dehydrated, and embedded in Spurr's medium (13, 22).

The papillary muscle is ideally suited for stereologic and morphometric study because, as previously discussed (22, 23), in its midregion the cardiocytes and capillaries all follow the long axis of the muscle and can be reliably examined in any selected orientation. The myocardial free wall, in contrast, presents a number of problems in determining its relative fiber orientation (24). Use of the left ventricular anterior papillary muscle also ensured that the same tissue was used from each heart.

Four blocks of tissue were randomly selected from each animal. Two were sectioned in longitudinal orientation (parallel to the long axis of cardiocytes and capillaries), and two were sectioned in transverse orientation (at right angle to this axis). Thick sections (1 μm) for light microscopy were cut, stained with toluidine blue, and examined at ×1250 with an Olympus BHS microscope. Each block, if necessary, was reoriented until the proper orientation was achieved. These thick sections were used for the measurement of cardiocyte cross-sectional area, tissue composition, and capillary distribution as described below. Thin sections (70 nm) were cut from the same blocks and stained with uranyl acetate and lead citrate. Photomicrographs were taken with a JEOL 100s transmission electron microscope at an initial magnification of ×3224, enlarged ×2.85, and used for the measurement of cardiocyte composition.

Quantitative Analysis. Morphometric and stereologic analysis employed a planimeter/digitizing tablet (Carl Zeiss, Thornwood, NY) interfaced with a microcomputer for data capture and analysis. Light microscopic measurements were made through an Olympus BHS microscope equipped with a sidearm lens which superimposed the image of the planimetry cursor and/or a digitizing grid over the image of the tissue. Stereologic analysis of ultrastructural composition was done with a grid placed directly over the electron micrographs. The theoretical foundations for these techniques (25, 26) are beyond the scope of this report, but their applications to myocardial analysis are well established and have been previously discussed (22, 23). All samples were identified by animal numbers which did not specify the experimental group to which each belonged.

Mean cross-sectional area was selected as an index of cardiocyte size because it can be reliably measured and is a sensitive indicator of changes in cell size during myocardial remodeling in the adult animal (22, 23). This was determined at ×1250 from transversely sectioned tissue by integrating tracings of the periphery of each cell. Only cardiocytes containing a nucleus were included to ensure that measurements were taken near the midpoint of each cylindrical cell, and all nucleated cells within a microscopic field were measured. Adjacent fields were examined until at least 50 cells from each of two blocks of tissue were measured, and a mean value was calculated for each animal.

Capillary diameter and numerical density were also measured at ×1250 from each of two transversely sectioned blocks of tissue per animal. Within a defined area (*A*) of 10,460 um^2, the total number (*N*) of capillaries were counted regardless of orientation to calculate their numerical density (ND), where ND = N/A. Nonoverlapping microscopic fields were examined until at least 200 capillaries had been counted in each block. Within each field, capillary profiles cut in cross-section were identified by endothelial symmetry, and their diameters measured with the planimeter. Mean density and diameter values were then calculated for each animal.

The relative volume densities of cardiocytes, extracellular matrix, and capillaries were determined by point-counting stereology (25, 26) using a 609-point grid superimposed over the image of the tissue at ×1250. The volume density of each component (*V*) relative to total tissue volume (*Vt*) was calculated as Vx/Vt = Px/Pt where *Px* and *Pt* are, respectively, the number of points falling over the component in question and the total number of points falling over the tissue. Two blocks each of longitudinally and transversely sectioned tissue were examined for each animal, and measurements were taken from three random

nonoverlapping fields in each block. A mean value for each tissue component in each animal was then calculated.

The relative volume densities of myofibrils, mitochondria, nucleus, and free cytoplasm relative to total cellular volume were calculated in the same way as Vx/Vt = Px/Pt using a 165-point grid placed over electron micrographs printed at a final magnification of ×9188. Two blocks each of transversely and longitudinally sectioned tissue from each rat were included, and five random areas from each block were photographed and used for analysis.

Since the dimensions of all measured tissue and cardiocyte components perpendicular to the section face far exceeded section thickness, the penetration factors (27) and consequent errors due to the Holmes effect (28) were negligible and were not corrected for. Similarly, the parallel organization of cardiocytes and capillaries within the papillary muscle allowed orientation of the tissue easily exceeding that necessary for stereologic analysis of cardiac muscle (29), obviating corrections for anisotropy. Factors of 1.03 to 1.08 to correct for section compression were calculated and applied as described by Anversa *et al.* (30).

Statistical Analysis. Each group of diabetic (alloxan injected) rats had an age-matched nondiabetic (saline injected) control group, and each insulin treated diabetic group had an age-matched saline treated diabetic control group. A two-tailed, nonpooled, unpaired Student's *t*-test was used to compare each value between the appropriate experimental and control groups.

In order to analyze the capacity of insulin replacement to prevent or reverse structural changes, measurements from insulin treated diabetic animals were also compared with those from nondiabetic control rats. Analysis of variance (ANOVA) revealed no significant differences among the six, 12, and 26 week nondiabetic control groups in any of the morphometric or stereologic analysis measurements, so a mean normal value was calculated for each parameter. A one-way ANOVA was then used to compare ITP or ITR groups and this pooled normal control, followed by a Newman-Kuels multiple comparison test when indicated by a $P \leq 0.05$.

Results

Evaluation of the Experimental Model. Table I summarizes the sacrifice weights, rate of weight gain, and blood glucose levels for the animals in this study. Nondiabetic control rats, as expected, had normal levels of blood glucose. Their weight gain was initially greater than 35 g per week but decreased with age as they approached adult weights. Untreated or saline-

Table I. Characteristics of the Experimental Model

Experimental group	(*n*)	Sacrifice weight (g)	Weight change per week (g)		Blood glucose (m*M*)	
			Before treatment	After treatment	Before treatment	After treatment
No treatment:						
6-Wk diabetic	8	192.8 ± 9.4*	1.65 ± 3.24*		26.96 ± 3.53*	
6-Wk nondiabetic	7	394.6 ± 44.7	36.10 ± 5.87		5.57 ± 0.45	
12-Wk diabetic	7	209.3 ± 44.4*	1.67 ± 3.48*		24.69 ± 2.22*	
12-Wk nondiabetic	8	487.0 ± 40.9	26.38 ± 3.20		5.43 ± 0.38	
26-Wk diabetic	7	201.1 ± 37.8*	1.30 ± 1.53*		25.49 ± 2.89*	
26-Wk nondiabetic	7	589.7 ± 91.1	15.81 ± 3.70		5.40 ± 0.63	
Prevention:						
6-Wk insulin-treated	7	369.7 ± 22.6*		34.11 ± 3.95*	21.16 ± 3.05	5.34 ± 1.25*
6-Wk saline-treated	6	169.2 ± 27.9		1.83 ± 4.13	28.83 ± 2.20	28.33 ± 2.10
12-Wk insulin-treated	7	441.9 ± 41.8*		22.84 ± 3.48*	25.51 ± 3.53	6.90 ± 0.80*
12-Wk saline-treated	6	205.8 ± 11.0		2.65 ± 1.04	25.85 ± 2.22	25.25 ± 3.31
26-Wk insulin-treated	8	524.0 ± 23.1*		13.94 ± 1.28*	22.36 ± 4.64	5.44 ± 0.34*
26-Wk saline-treated	6	241.7 ± 19.0		3.08 ± 0.80	23.22 ± 3.43	23.37 ± 1.14
Reversal:						
6-Wk insulin-treated	6	366.2 ± 28.2*	7.60 ± 3.04	20.32 ± 2.10*	25.52 ± 2.37	6.20 ± 1.30*
6-Wk saline-treated	7	213.6 ± 26.3	2.00 ± 2.17	3.94 ± 1.88	25.06 ± 2.23	24.33 ± 2.03
12-Wk insulin-treated	6	415.8 ± 13.1*	6.70 ± 2.70	13.92 ± 2.88*	26.30 ± 5.32	5.53 ± 0.75*
12-Wk saline-treated	6	266.8 ± 51.1	4.67 ± 3.88	3.67 ± 2.82	27.65 ± 5.05	25.88 ± 3.31
26-Wk insulin-treated	8	511.6 ± 31.2*	3.54 ± 1.37	11.86 ± 1.71*	24.13 ± 1.69	6.41 ± 0.90*
26-Wk saline-treated	6	242.8 ± 20.3	2.33 ± 1.12	2.07 ± 0.75	25.82 ± 1.90	25.03 ± 1.57

Body weight, rate of weight gain, and blood glucose levels of age-matched diabetic and nondiabetic rats and of age-matched insulin-treated and saline-treated diabetic rats. Insulin or saline treatment began three days after induction of diabetes in the Prevention groups, and 12 weeks after induction of diabetes in the Reversal groups. All values are expressed as $\bar{x} \pm$ SD. *$P \leq 0.01$ by Student's *t* test for comparisons of diabetic versus nondiabetic groups and of insulin-treated versus saline-treated diabetic groups.

treated diabetic animals, in contrast, remained markedly hyperglycemic and gained little weight throughout the study.

Insulin treatment begun either three days (ITP) or 12 weeks (ITR) after induction of diabetes restored both blood glucose and rate of weight gain to normal. Plasma glucose concentrations measured in ITR rats at 2-hr intervals (Fig. 1) verified that our procedure of semidaily injections of mixed insulins maintained a stable level of euglycemia throughout the day. These values in the untreated diabetic animals, in contrast, reflected the typical eating pattern of the rat, significantly rising at night when most of the food is consumed and falling during the day, when the animal eats little food (20).

Untreated and saline-treated diabetic animals consistently had markedly elevated urine glucose and ketone levels above the dipstick maxima of 1 g/dl [55.6 m*M*] glucose and 250 mg/dl [23.1 m*M*] acetoacetate. Water consumption and urine output were markedly elevated. Proteinuria was present only in trace amounts, if at all, in these animals. Glucosuria disappeared within one to two days of both ITP and ITR, with loss of ketonuria approximately one day later. Urine glucose, ketones, and protein were all absent in nondiabetic control rats throughout the study.

Measurement of daily food consumption in age-matched diabetic and nondiabetic animals over a three-week period confirmed that the lack of weight gain in diabetes was not due to starvation. Diabetic animals, in fact, ate 64% more food than did control rats (51.0 ± 2.6 g/d vs 31.1 ± 1.7 g/d, $\bar{x}$ ± SD, $P < 0.001$, $n = 4$ per group).

Cataracts were not seen in any nondiabetic rats in this study but developed within 12 weeks in all animals in the untreated or saline-treated diabetic groups. These could be prevented by early insulin replacement but could not be reversed if insulin treatment was delayed for 12 weeks. Diabetic animals also had a striking loss of subcutaneous fat, and a loss of retroperitoneal fat was also evident at sacrifice. Insulin treatment, ITP or ITR, maintained or redeposited adipose tissue at both sites.

Gross Examination. Neither diabetes nor insulin treatment affected the gross appearance of the heart. Diabetic animals retained the same amount of epicardial fat accompanying the coronary macrovasculature as did their age-matched nondiabetic controls, even though subcutaneous and retroperitoneal fat were lost.

As shown in Table II, heart weight after six weeks of diabetes was significantly less than in age-matched control animals and remained so throughout the study, but the increased heart weight:body weight ratios in these animals demonstrate that the effects of insulin deficiency on overall growth were even more pronounced. ITP and ITR maintained or restored both heart weights and heart weight:body weight ratios, while saline treatment, as expected, had no effect on

Table II. Effects of Diabetes and Insulin Treatment on Heart Weight

Experimental group	(*n*)	Heart weight at sacrifice (g)	Heart weight per body weight (g/kg)
No treatment:			
6-Wk diabetic	8	0.56 ± 0.04*	2.90 ± 0.14*
6-Wk nondiabetic	7	0.99 ± 0.11	2.52 ± 0.15
12-Wk diabetic	7	0.67 ± 0.12*	3.36 ± 0.30*
12-Wk nondiabetic	8	1.08 ± 0.09	2.22 ± 0.16
26-Wk diabetic	7	0.71 ± 0.14*	3.61 ± 0.80*
26-Wk nondiabetic	7	1.15 ± 0.06	1.97 ± 0.46
Prevention:			
6-Wk insulin-treated	7	0.90 ± 0.16*	2.37 ± 0.40*
6-Wk saline-treated	6	0.59 ± 0.15	3.43 ± 0.53
12-Wk insulin-treated	7	0.98 ± 0.11*	2.23 ± 0.26*
12-Wk saline-treated	6	0.72 ± 0.13	3.52 ± 0.61
26-Wk insulin-treated	8	1.17 ± 0.06*	2.23 ± 0.14*
26-Wk saline-treated	6	0.82 ± 0.10	3.39 ± 0.36
Reversal:			
6-Wk insulin-treated	6	0.97 ± 0.09*	2.67 ± 0.32*
6-Wk saline-treated	7	0.72 ± 0.13	3.32 ± 0.32
12-Wk insulin-treated	6	1.00 ± 0.12	2.39 ± 0.25*
12-Wk saline-treated	6	0.86 ± 0.07	3.30 ± 0.57
26-Wk insulin-treated	8	1.18 ± 0.08*	2.30 ± 0.05*
26-Wk saline-treated	6	0.74 ± 0.05	3.04 ± 0.10

Absolute and relative heart weights of age-matched diabetic and nondiabetic rats and of age-matched insulin-treated and saline-treated diabetic rats. Insulin or saline treatment began three days after induction of diabetes in the Prevention groups, and 12 weeks after induction of diabetes in the Reversal groups. All values are expressed as $\bar{x}$ ± S.D. *$P \leq 0.01$ by Student's *t* test for comparisons of diabetic versus nondiabetic groups and of insulin-treated versus saline-treated diabetic groups.

the diabetic changes. Right and left ventricular mass were equally affected by both diabetes and insulin treatment (Fig. 2).

Cardiocyte Cross-Sectional Area. The mean cardiocyte cross-sectional areas for all experimental animals are shown in Figure 3. A decrease of 12% ($P \leq 0.01$) was noted after six weeks of untreated diabetes, which progressed to 24% after 12 weeks but remained stable thereafter. No changes in cellular cross-sectional area were evident with age in the nondiabetic control animals.

ITP maintained cardiocyte sizes indistinguishable from those of nondiabetic rats and significantly larger than those of diabetic animals injected with saline (Fig. 3). Long-term ITR produced a progressive reversal, evident after six weeks and complete by 26 weeks. Saline-treated control animals for the last of these groups, which were insulin deficient for a total of 38 weeks (12 weeks of untreated diabetes plus 26 weeks of saline treatment), had a mean cardiocyte cross-sectional area less than 8% below that of the 12 week diabetic group, confirming that further decreases were minimal as the diabetes progressed.

Tissue Composition. Untreated diabetes produced a significant increase in extracellular matrix, shown in the stereologic analysis presented in Figure 4. This increase occurred at the expense of both cardiac muscle cells and capillaries, although the relatively large variance in the latter resulted in changes which were not statistically significant until 26 weeks.

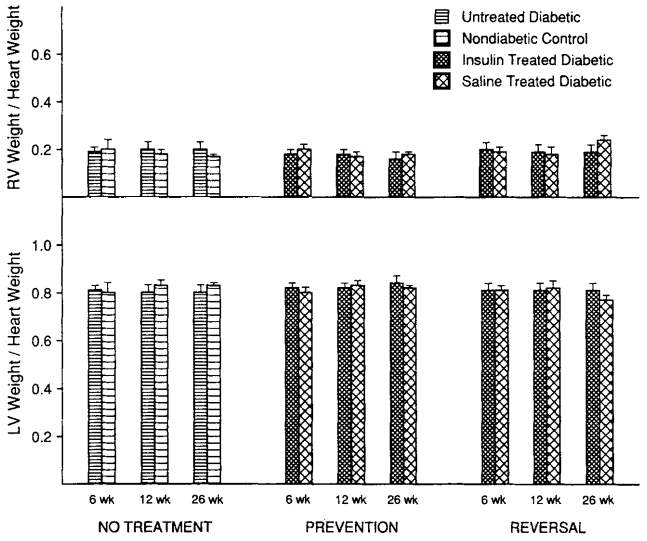

Figure 2. Right ventricular (RV) and left ventricular plus septum (LV) weights relative to total heart weight are compared between age-matched diabetic and nondiabetic rats and between age-matched insulin-treated and saline-treated diabetic rats. Insulin or saline treatment began three days after induction of diabetes in the Prevention groups, and 12 weeks after induction of diabetes in the Reversal groups. The number of animals in each group is presented in Table I, and all values are expressed as $\bar{x} \pm$ S.D. Comparisons of diabetic versus nondiabetic groups and of insulin-treated versus saline-treated diabetic groups by Student's t test revealed no significant differences at $P \leq 0.01$.

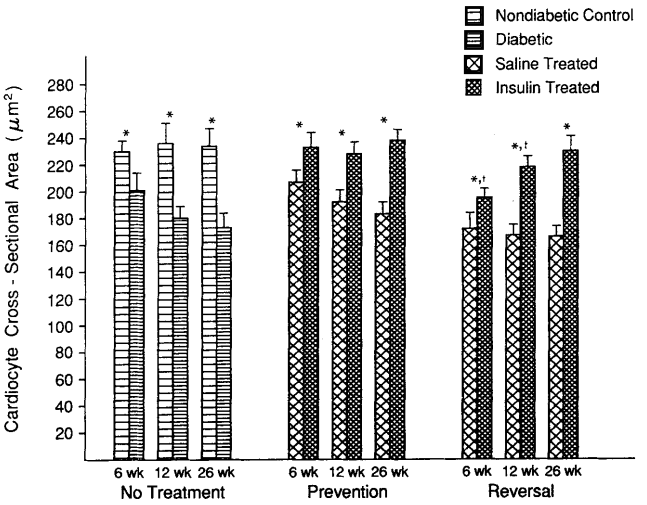

Figure 3. Cardiocyte cross-sectional areas of age-matched diabetic and nondiabetic rats and of age-matched insulin-treated and saline-treated diabetic rats. Insulin or saline treatment began three days after induction of diabetes in the Prevention groups, and 12 weeks after induction of diabetes in the Reversal groups. The number of animals in each group is presented in Table I, and all values are expressed as $\bar{x} \pm$ SD. $^*P \leq 0.01$ by Student's t test for comparison of diabetic versus nondiabetic groups and of insulin-treated versus saline-treated diabetic groups. Comparison of nondiabetic versus insulin treated diabetic groups by ANOVA was followed by Newman-Kuels multiple comparison test; $\dagger P \leq 0.01$ relative to nondiabetic values.

The deposition of extracellular matrix progressed to the extent that its relative volume density had tripled after 26 weeks of diabetes, while those of the cardiocytes and capillaries had decreased 15% and 30%, respectively.

Prompt insulin replacement again prevented the effects of diabetes on myocardial composition (Fig. 5). The relative volume densities (*RVD*) of cardiocytes and capillaries in these animals remained unchanged from the nondiabetic values presented in Figure 4, while the *RVD* of the extracellular matrix even decreased slightly after 26 weeks of treatment. Changes

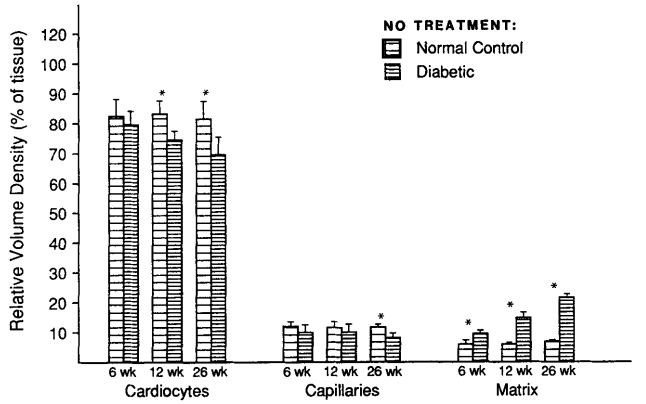

Figure 4. Histologic composition of the myocardium is compared between age-matched diabetic and nondiabetic rats. The number of animals in each group is presented in Table I. All values are expressed as $\bar{x} \pm$ SD. $^*P \leq 0.01$ by Student's t test for comparisons of diabetic versus nondiabetic controls.

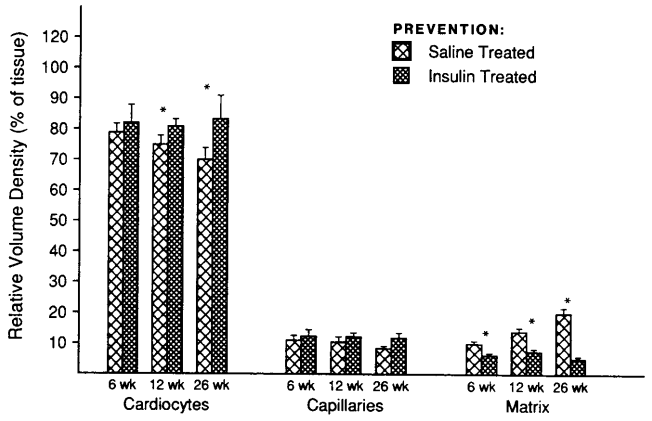

Figure 5. Histologic composition of the myocardium is compared between age-matched diabetic animals in which insulin or saline injections began three days after induction of diabetes. The number of animals in each group is presented in Table I. All values are expressed as $\bar{x} \pm$ SD. *$P \leq 0.01$ by Student's t test for comparisons of insulin-treated versus saline-treated diabetic groups. Comparison of nondiabetic (presented in Fig. 4) versus insulin treated diabetic groups by ANOVA revealed no significant differences in any of the measured parameters at $P \leq 0.01$.

in the control groups of saline-treated diabetic rats paralleled those which occurred in the untreated diabetic groups.

Delayed insulin treatment restored the *RVDs* of cardiocytes and capillaries within six weeks to values not significantly different from those in nondiabetic rats and maintained them thereafter (Fig. 6). The *RVD* of extracellular matrix, in contrast, remained 70% greater than that of nondiabetic animals even after 26 weeks of treatment, more at the expense of capillaries (86.3% of nondiabetic) than of cardiocytes (95.6% of nondiabetic). Thus, while insulin treatment prevented

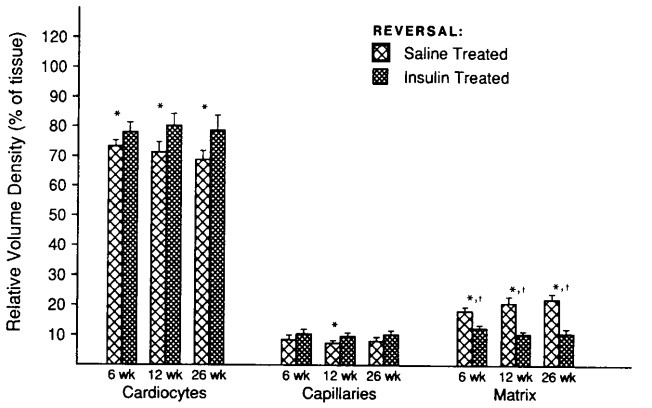

Figure 6. Histologic composition of the myocardium is compared between age-matched diabetic animals in which insulin or saline injections began 12 weeks after induction of diabetes. The number of animals in each group is presented in Table I. All values are expressed as $\bar{x} \pm$ SD. *$P \leq 0.01$ by Student's t test for comparisons of insulin treated versus saline treated diabetic groups. Comparison of nondiabetic versus insulin-treated diabetic groups by ANOVA was followed by Newman-Kuels multiple comparison test; †$P \leq 0.01$ relative to nondiabetic values presented in Figure 4.

diabetic changes in myocardial composition when begun early, it could not completely restore normal histoarchitecture once they had occurred.

It is important to note that while myocardial damage in the diabetic rats occurred in a progressive pattern, replacement fibrosis was not observed even after the prolonged periods of diabetes. The increased extracellular material instead consisted of diffuse perivascular and intercardiocyte deposition of nonfibrillar matrix. Remnants of cellular necrosis, either cardiocyte or endothelial cell, were rarely observed in tissue from either diabetic or nondiabetic animals, nor was leukocytic inflammation evident.

Capillary Diameter and Density. As shown in Table III, planimetry revealed that the mean capillary diameter had progressively decreased by 11% after 12 weeks and 22% after 26 weeks of untreated diabetes (both $P \leq 0.01$). Stereologic analysis also revealed a significant ($P \leq 0.01$) progressive decline in capillary density with continued diabetes, reaching 77% of the value in nondiabetic age-matched controls after 26 weeks. Comparisons with the saline-treated control group for ITR studies, in which the animals remained diabetic for 38 weeks (12 weeks untreated plus 26 weeks of saline treatment), indicated that the changes in capillary density and diameter were essentially complete within the 26 week interval of this study.

ITP retained normal capillary diameter and prevented the loss of capillary density over the interval of this study. ITR restored capillary diameter to nondiabetic values within six weeks and quickly, but not completely, reversed the change in capillary density. While the density values in the ITR groups represent a return to greater than 90% of those measured in nondiabetic control animals, the differences remained statistically significant, reflecting the increased *RVD* of myocardial extracellular matrix in these animals.

Cardiocyte Ultrastructural Composition. The ultrastructural appearance of cardiocytes from nondiabetic, untreated, and insulin treated diabetic rats is shown in Figure 7. Stereologic analysis revealed that the increased *RVD* of free cytoplasm in cells from untreated (Fig. 8) and saline treated (Fig. 9) diabetic animals initially occurred by loss of myofibrils, followed by decreased *RVD* of mitochondria. After 26 weeks of untreated diabetes, free cytoplasm had quadrupled to 20% of cardiocyte volume while myofibrils and mitochondria showed losses of 23% and 18% respectively (all $P \leq 0.01$). The modestly increased nuclear *RVD* in diabetic rats reflects the decreased cardiocyte size (Fig. 3) while nuclear volume was maintained.

Similar to its effect on tissue composition, ITP (Fig. 9) prevented changes in cardiocyte ultrastructure at all intervals studied. When delayed (Fig. 10), insulin treatment eventually restored normal cardiocyte ultra-

Table III. Capillary Diameter and Density

Experimental group	(*n*)	Capillary diameter (μm)	Capillary density (no./mm)
No treatment:			
6-Wk diabetic	8	5.79 ± 0.37	3292 ± 217*
6-Wk nondiabetic	7	6.27 ± 0.54	3646 ± 147
12-Wk diabetic	7	5.57 ± 0.43*	3053 ± 263*
12-Wk nondiabetic	8	6.29 ± 0.37	3591 ± 204
26-Wk diabetic	7	5.12 ± 0.71*	2687 ± 173*
26-Wk nondiabetic	7	6.58 ± 0.55	3481 ± 229
Prevention:			
6-Wk insulin-treated	7	6.17 ± 0.49	3477 ± 186
6-Wk saline-treated	6	5.79 ± 0.33	3422 ± 220
12-Wk insulin-treated	7	6.23 ± 0.48	3582 ± 214*
12-Wk saline-treated	6	5.30 ± 0.33	3090 ± 186
26-Wk insulin-treated	8	6.36 ± 0.23*	3501 ± 133*
26-Wk saline-treated	6	5.44 ± 0.31	2635 ± 161
Reversal:			
6-Wk insulin-treated	6	6.55 ± 0.56*	3315 ± 123*
6-Wk saline-treated	7	5.32 ± 0.24	2855 ± 138
12-Wk insulin-treated	6	6.21 ± 0.35*	3354 ± 172*
12-Wk saline -treated	6	5.19 ± 0.37	2709 ± 204
26-Wk insulin-treated	8	6.27 ± 0.37*	3346 ± 200*,†
26-Wk saline-treated	6	5.20 ± 0.22	2673 ± 227

Capillary diameter and density in the myocardium of diabetic and nondiabetic rats and age-matched insulin-treated and saline-treated diabetic rats. Insulin or saline treatment began three days after induction of diabetes in the Prevention groups, and 12 weeks after induction of diabetes in the Reversal groups. All values are expressed as $\bar{x}$ ± S.D. *$P \leq 0.01$ by Student's *t* test for comparisons of diabetic versus nondiabetic groups and of insulin-treated versus saline-treated diabetic groups. Comparison of nondiabetic versus insulin-treated diabetic groups by ANOVA was followed by Newman-Kuels multiple comparison test; †$P \leq 0.01$ relative to nondiabetic values.

structure, although increased free cytoplasm at the expense of myofibrils persisted through the first six weeks. Similar to capillary changes noted above, the saline-treated control animals which were insulin deficient for 38 weeks showed that little further change in cardiocyte composition occurred if the diabetes was prolonged.

Discussion

In this study, I have quantitatively defined the striking changes of myocardial structure which occur in insulin-dependent diabetes mellitus and have, for the first time, stereologically correlated the effects of chronic diabetes and insulin replacement on the different components of the myocardial tissue to provide structural information on which compensatory or degenerative changes in the function of the diabetic heart can be interpreted.

The model of alloxan diabetes in the rat selected for this study produces a constellation of both direct and indirect changes which closely mimic the disease in humans and has, consequently, been widely used by many investigators for experimental studies of diabetes. Reversibility of structural (13, 20), biochemical (21, 31), and physiologic (32, 33) sequelae together with restored growth rates upon insulin treatment confirm that alloxan diabetes represents insulin deficiency rather than either alloxan toxicity or insulin resistance. The observation that diabetic rats were markedly hyperphagic confirms that the lack of weight gain in diabetic animals is not due to starvation.

The progressive decrease in capillary size and number observed in this study have particularly significant physiological implications for the diabetic heart. Tomanek *et al.* (34) have shown that capillary density, and to a lesser extent capillary diameter, are the primary determinants of capillary surface area for the exchange of materials between the myocardial interstitium and the blood. Thus, these decreases, together with the endothelial thickening which also occurs (13), restrict the supply of oxygen and metabolic substrates to the blood and the clearance of metabolic byproducts.

Decreased capillary density within the myocardium also limits its perfusion during conditions which require full use of the coronary reserve. In diabetic patients, exercise has unmasked decreased fractional shortening and shortening velocity (8), reduced ejection fraction (9), and electrocardiographic changes typical of ischemia (35) which were not evident when the patients were at rest. Abnormalities of left ventricular end diastolic volume, stroke volume, and ejection

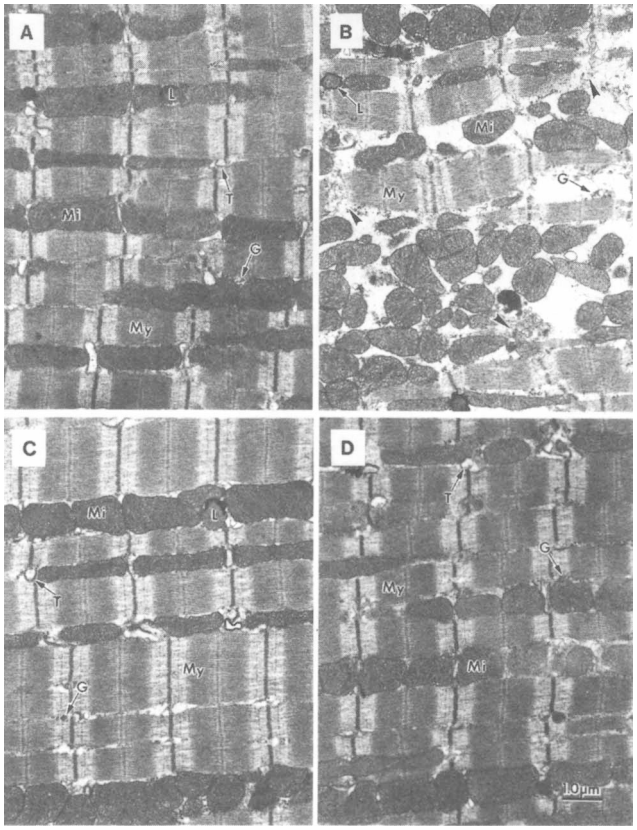

Figure 7. Ultrastructural appearance of cardiocytes from 12 week nondiabetic (A), 12-week diabetic (B), 12-week insulin treatment–prevention (C), and 12-week insulin treatment–reversal (D) rats. Diabetes resulted in a marked loss and disorganization of myofibrils (My), leaving areas of free cytoplasm and grouped intermyofibrillar mitochondria (Mi) which appear somewhat irregular in shape but otherwise ultrastructurally normal. Myofibrillar disruption is particularly evident at Z-lines (arrowheads), and transverse tubules (T) are much less evident than in normal tissue. Glycogen (G) and lipid (L) storage appears unaffected by diabetes. Insulin treatment begun three days after induction of diabetes prevented these ultrastructural sequelae, and insulin treatment begun 12 weeks after induction, when the changes shown in B were present, restored normal cytoarchitecture.

fraction have also been elicited in diabetic patients in response to the cold pressor test (36). Similarly, diminished myocardial function during increased work loads has been demonstrated in isolated perfused hearts from diabetic animals (37, 38), and an impaired ability of the diabetic dog heart to respond to angiotensin-induced afterload has been demonstrated (39).

The unchanged heart weights shown in Table II for diabetic animals actually reflect the dynamic balance of increased extracellular mass approximately compensating for loss of capillary and myocyte mass. Although an increase in the ratio of extracellular to cardiocyte mass has also been reported in myocardial hypertrophy induced by pressure, but not volume, overloading (23), the situations are not the same. Unlike hypertrophy, where this ratio reflects disproportionate growth of both components, in diabetes the

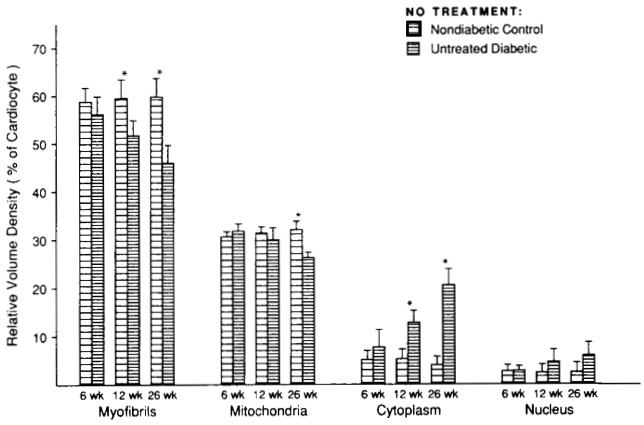

Figure 8. Ultrastructural composition of cardiocytes is compared between age-matched diabetic and nondiabetic rats. The number of animals in each group is presented in Table I. All values are expressed as $\bar{x} \pm$ SD. $^*P \leq 0.01$ by Student's t test for comparisons of diabetic versus nondiabetic controls.

change in cardiocyte size confirms that cellular mass is decreasing in both absolute and relative terms while extracellular material is being deposited. This is similar to changes which occur after mechanical unloading (40), indicating that the process may essentially be one of atrophy. Prevention or reversal of changes by insulin replacement and by pancreatic transplantation (41) are also similar to reversal of atrophy by reimposition of mechanical load (22), raising the intriguing possibility that these processes may have some biochemical mechanisms in common.

The presence of excessive amounts of extracellular material is a common feature of diabetic cardiomyopathy (5–7) and has been linked (2, 14) to increased stiffness and decreased diastolic compliance. Replace-

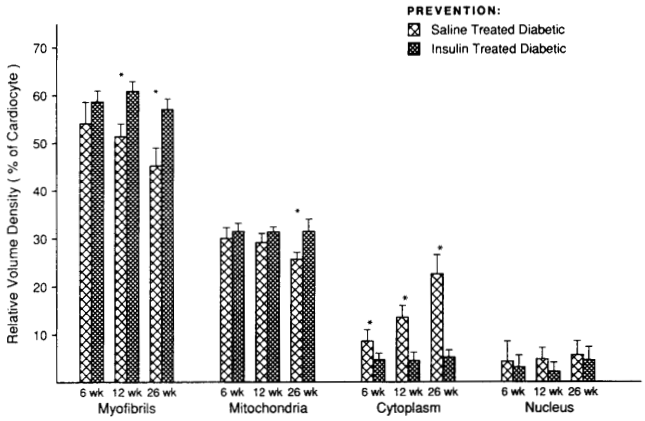

Figure 9. Ultrastructural composition of cardiocytes is compared between age-matched diabetic rats in which insulin or saline injections began three days after induction of diabetes. The number of animals in each group is presented in Table I. All values are expressed as $\bar{x} \pm$ SD. $^*P \leq 0.01$ by Student's t test for comparisons of insulin-treated versus saline-treated diabetic groups. Comparison of nondiabetic (presented in Figure 8) versus insulin-treated diabetic groups by ANOVA revealed no significant differences in any of the measured parameters at $P \leq 0.01$.

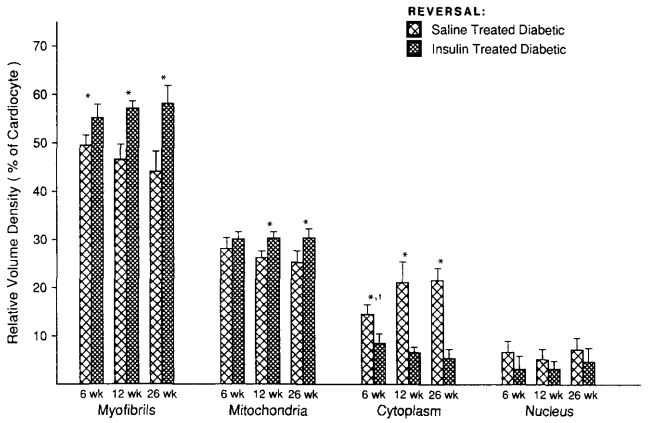

Figure 10. Ultrastructural composition of cardiocytes is compared between age-matched diabetic rats in which insulin or saline injections began 12 weeks after induction of diabetes. The number of animals in each group is presented in Table I. All values are expressed as $\bar{x} \pm$ SD. *$P \leq 0.01$ by Student's t test for comparisons of insulin treated versus saline treated diabetic groups. Comparison of nondiabetic versus insulin treated diabetic groups by ANOVA was followed by Newman-Kuels multiple comparison test; † = $P \leq 0.01$ relative to nondiabetic values presented in Figure 8.

ment fibrosis and gross scarring are often, although not always (5, 6), present in the human diabetic myocardium, but not in experimentally diabetic animals (13, 41) unless hypertension is also present (42).

Extracellular edema caused by altered capillary permeability in diabetic tissues probably also plays a role in the increased relative volume density of the extracellular matrix. However, the extensive and highly organized network of myocyte-to-myocyte and myocyte-to-capillary collagen struts demonstrated by Borg *et al.* (43) make it unlikely that edema could account for more than a small fraction of the increased extracellular material without cellular deformation, which was not present. Nonetheless, even a small degree of edema would compromise matrix function by altering its tensile and compressive properties.

Intracellular edema of the cardiocytes, in contrast, is more likely to be a factor in the changes we observed. The increased relative volume densities of free cytoplasm shown in Figures 8 through 10 at least partially reflect increased intracellular osmolarity due to the metabolic abnormalities characteristic of diabetes. The selective permeability of the cardiocyte sarcolemma is also compromised in diabetes (44), further predisposing the cells to edema.

However, it is important to note that these occurred in cardiocytes which were simultaneously decreasing in size, so the presence of edema would mean an absolute loss of myofibrils and mitochondria even greater than indicated by the stereologic analysis of ultrastructural composition. The 23% and 18% decreases in *RVDs* of myofibrils and mitochondria, respectively, after 26 weeks of diabetes together with a 26% decrease in mean cardiocyte cross-sectional area over the same period indicate absolute decreases of over 40% in the mass of each of these two cellular components. Since these are the primary energy consuming and energy producing structures within the contracting cardiocyte, this parallel loss indicates that it continues to balance these two processes even though mitochondrial function is compromised in diabetes (44). Reversal by insulin subsequently involved both correction of the osmotic abnormalities and restoration of myofibrillar and mitochondrial mass.

The observation that the ultrastructural appearance of the mitochondria was unchanged in intact cells of diabetic animals does not agree with reports from other investigators (12, 16) which described mitochondrial swelling and disruption. These reports, however, may in part reflect artifact due to delayed fixative penetration since the tissues were fixed by immersion. All tissues in this study, in contrast, were immediately arrested in diastole and rapidly fixed by vascular perfusion, and disrupted mitochondria were limited to cardiocytes in which sarcolemmal integrity was lost. Normal mitochondrial ultrastructure is also evident in perfusion-fixed myocardial tissue from the spontaneously diabetic BB rat presented by McGrath and McNeill (15) in which mitochondria were more heterogeneous in shape but otherwise uninvolved, even in areas of extensive free cytoplasm. The observation that in vivo levels of myocardial ATP are maintained in chronically diabetic rats (45) also supports the maintenance of mitochondrial integrity.

Nonetheless, fixation artifact cannot fully account for differences in mitochondrial appearance, since even in studies using immersion fixation the mitochondria in diabetic tissue show more damage than do those in nondiabetic tissue. The observation that the mitochondrial membrane is abnormally permeable in diabetic myocardium (44), and that isoproterenol-induced damage of myocardial mitochondria was much more severe in diabetic than in nondiabetic rabbits (46) indicate that myocardial mitochondria from diabetic animals remain intact *in vivo* but are more susceptible to injury from a number of insults and are more likely to be damaged during preparation for microscopic examination.

In interpreting the results of this or any other study of diabetic cardiomyopathy, it is important to bear in mind that all diabetic sequelae must be considered a mosaic of both primary and secondary pathology. While insulin deficiency produces direct biochemical changes in the myocardium, the diabetic heart must often also adapt to altered and fluctuating substrate availability, systemic and renal hypertension, and autonomic neuropathy. These occur even with good clinical management of diabetes, and together with primary effects of the disease on the cardiocytes, their interstitium, and their vascular supply,

they underlie the clinically frustrating observation that heart disease remains markedly elevated in the diabetic population even with the best protocols of treatment available.

This work was supported by the Minnesota Affiliate of the American Heart Association, the Minnesota Affiliate of the American Diabetes Association, and the Hormel Foundation. I would like to acknowledge Wayne H. Anderson, Julie C. Baker, and Stacey A. Kamoss for their excellent technical assistance throughout this project, Dr. Brant Deppa for statistical advice, and the assistance of Carmen Perleberg for the preparation of this manuscript.

1. Kannel WB, McGee DL. Diabetes and cardiovascular disease: The Framingham study. JAMA **241**:2035–2038, 1979.
2. Regan TJ, Lyons MM, Ahmed SS, Levinson GE, Oldewurtel HA, Ahmad M, Haider B. Evidence for cardiomyopathy in familial diabetes mellitus. J Clin Invest **60**:885–899, 1977.
3. Seneviratne BIB. Diabetic cardiomyopathy: The preclinical phase. Br Med J **1**:1444–1446, 1977.
4. Fisher BM, Gillen G, Lindop GBM, Dargie HJ, Frier BM. Cardiac function and coronary arteriography in asymptomatic Type 1 (insulin-dependent) diabetic patients: Evidence for a specific diabetic heart disease. Diabetologia **29**:706–712, 1986.
5. Sutherland CG, Fisher BM, Frier BM, Dargie HJ, Mores IAR, Lindops GBM. Endomyocardial biopsy pathology in insulin-dependent diabetic patients with abnormal ventricular function. Histopathology **14**:593–602, 1989.
6. Das AK, Das J, Chandrasekar S. Specific heart muscle disease in diabetes: A functional structural correlation. Int J Cardiol **17**:299–302, 1987.
7. Rubler S, Dlugash J, Yuceoglu Y, Kumral T, Branwood A, Grishman A. A new type of cardiomyopathy associated with diabetic glomerulosclerosis. Am J Cardiol **30**:595–602, 1972.
8. Baum VC, Levitsky LL, Englander RM. Abnormal cardiac function after exercise in insulin-dependent diabetic children and adolescents. Diab Care **10**:319–323, 1987.
9. Margonato A, Gerundini P, Vicedomini G, Gilardi MC, Pozza G, Fazio F. Abnormal cardiovascular response to exercise in young asymptomatic diabetic patients with retinopathy. Am Heart J **112**:554–560, 1986.
10. Paulson DJ, Kopp SJ, Peace DG, Tow JP. Myocardial adaptation to endurance exercise training in diabetic rats. Am J Physiol **252**:R1073–R1081, 1987.
11. DeBlieux PM, Barbee W, McDonough KH, Shepard RE. Exercise training improves cardiac performance in diabetic rats. Proc Soc Exp Biol Med **203**:209–213, 1993.
12. Koltai MZ, Balogh I, Wagner M, Pogatsa C. Diabetic myocardial alterations in ultrastructure and function. Exper Pathol **25**:215–221, 1984.
13. Thompson EW. Structural manifestations of diabetic cardiomyopathy in the rat and its reversal by insulin treatment. Am J Anat **182**:270–282, 1988.
14. Airaksinen J, Ikaheimo M, Kaila J, Linnaluoto M, Takkunen J. Impaired left ventricular filling in young female diabetics, an echocardiographic study. Acta Med Scand **216**:509–516, 1984.
15. McGrath GM, McNeill JH. Ultrastructural study of the effect of insulin dosage on the myocardium of spontaneously diabetic BB rats. Can J Physiol Pharmacol **65**:2212–2218, 1987.
16. Jackson CV, McGrath GM, Tahiliani AG, Vadlamudi RVSV, McNeill JH. A functional and ultrastructural analysis of experimental diabetic rat myocardium. Diabetes **34**:876–883, 1985.
17. Seager MJ, Singal PK, Orchard R, Pierce GN, Dhalla NS. Cardiac cell damage: A primary myocardial disease in streptozotocin-induced chronic diabetes. Br J Exp Pathol **65**:613–623, 1984.
18. Bakth S, Arena J, Lee W, Torres R, Haider B, Patel BC, Lyons MC, Regan TJ. Arrhythmia susceptibility and myocardial composition in diabetes. Influence of physical conditioning. J Clin Invest **77**:382–395, 1986.
19. Thompson EW, Baker JC, Kamoss SA, Anderson WH. The severity of diabetes is a major determinant of myocardial damage in the rat. Proc Soc Exp Biol Med **196**:230–233, 1991.
20. Thompson EW, Parks WC, Drake RL. Rapid alterations induced by insulin in hepatocyte ultrastructure and glycogen levels. Am J Anat **160**:449–460, 1981.
21. Drake RL, Parks WC, Thompson EW. Insulin stimulation of hepatic malic enzyme activity in normal and diabetic rats controlled by different regulatory processes. J Biol Chem **258**:6008–6010, 1983.
22. Thompson EW, Marino TA, Uboh CE, Kent RL, Cooper G. Atrophy reversal and cardiocyte redifferentiation in reloaded cat myocardium. Circ Res **54**:367–377, 1984.
23. Marino TA, Kent RL, Uboh CE, Fernandez E, Thompson EW, Cooper G. Structural analysis of pressure versus volume overload hypertrophy of cat right ventricle. Am J Physiol **249**:H371–H379, 1985.
24. McLean M, Prothero J. Determination of relative fiber orientation in heart muscle: Methodological problems. Anat Rec **232**:459–465, 1992.
25. Elias H, Hennig A, Schwartz DE. Stereology: Applications to biomedical research. Physiol Rev **51**:158–200, 1971.
26. Williams MA. Stereological techniques. In: Glauert AM, Ed. Practical Methods in Electron Microscopy. Vol. 6, Part 2: Quantitative Methods in Biology. Amsterdam: North Holland Press, pp5–84, 1977.
27. Loud AV, Anversa P, Giacomelli F, Wiener J. Absolute morphometric study of myocardial hypertrophy in experimental hypertension. Lab Invest **38**:586–596, 1978.
28. Weibel ER. Correction of systematic errors due to finite section thickness. In: Weibel E, Ed. Stereological Methods: Practical Methods for Biological Morphometry. New York: Academic Press, Vol. 1: pp139–150, 1979.
29. Olivetti G, Ricci R, Lagrasta C, Maniga E, Sonnenblick EH, Anversa P. Cellular basis of wall remodeling in long-term pressure overload-induced right ventricular hypertrophy in rats. Circ Res **63**:648–657, 1988.
30. Anversa P, Olivetti G, Melissari M, Loud AV. Morphometric study of myocardial hypertrophy induced by abdominal aortic stenosis. Lab Invest **40**:341–349, 1979.
31. Pollack PS, Malhotra A, Fein FS, Scheuer J. Effects of diabetes on cardiac contractile proteins in rabbits and reversal with insulin. Am J Physiol **251**:H448–H454, 1986.
32. Fein FS, Miller-Green B, Zola B, Sonnenblick EH. Reversibility of diabetic cardiomyopathy with insulin in rabbits. Am J Physiol **250**:H108–H113, 1986.
33. Downing SE. Restoration of coronary dilator action of adenosine in experimental diabetes. Am J Physiol **249**:H102–H107, 1985.
34. Tomanek RJ, Searls JC, Lachenbruch PA. Quantitative changes in the capillary bed during development, peak, and stabilized cardiac hypertrophy in the spontaneously hypertensive rat. Circ Res **51**:295–304, 1982.
35. Hume L, Oakley GD, Boulton AJ, Hardisty C, Ward JD. Asymptomatic myocardial ischemia in diabetes and its relationship to diabetic neuropathy: An exercise electrocardiography study in middle-aged diabetic men. Diab Care **9**:384–388, 1986.
36. Friedman HS, Sacerdote A, Bandu I, Jubay F, Herrera AG, Vasavada BC, Bleicher SJ. Abnormalities of the cardiovascular

response to cold pressor test in Type I diabetes. Correlation with blood glucose control. Arch Intern Med **144:**43–47, 1984.
37. Penparkul S, Schaible T, Yipintsoi T, Scheuer J. The effect of diabetes on performance and metabolism of rat hearts. Circ Res **47:**911–921, 1980.
38. Ingebretsen CG, Moreau P, Hawelu-Johnson C, Ingebretsen KR. Performance of diabetic rat hearts: Effects of anoxia and increased work load. Am J Physiol **239:**H614–H620, 1980.
39. Regan TJ, Khan MI, Jesrani MU, Oldewurtel HA, Ettinger PO. Alterations of myocardial function and metabolism in chronic diabetes mellitus. Rec Adv Stud Card Struct Metab **3:**169–178, 1973.
40. Tomanek RJ, Cooper G. Morphological changes in the mechanically unloaded myocardial cell. Anat Rec **200:**271–280, 1981.
41. Hayashi T, Kawamura K, Otsu I, Nozawa M. Effect of pancreatic transplantation on cardiovascular changes in diabetic rats: A qualitative and quantitative ultrastructural study. Trans Proc **22:**2027–2034, 1990.
42. Factor SM. Intramural pathology in the diabetic heart: Interstitial and microvascular alterations. Mt Sinai J Med **49:**208–214, 1982.
43. Borg TK, Caulfield JB. The collagen matrix of the heart. Fed Proc **40:**2037–2041, 1981.
44. Kuo TH, Moore KH, Giacomelli F, Wiener J. Defective oxidative metabolism of heart mitochondria from genetically diabetic mice. Diabetes **32:**781–787, 1983.
45. Gertz BJ, Haugaard ES. Effect of diabetes and fasting on the uridine triphosphate content and uridine kinase activity of rat cardiac and skeletal muscle. Metabolism **28:**358–362, 1979.
46. Bhimji S, McNeill JH. Isoproterenol-induced ultrastructural alterations in hearts of alloxan-diabetic rabbits. Gen Pharmacol **20:**479–485, 1989.